POLITECNICO DI TORINO
Repository ISTITUZIONALE

Causality-constrained interpolation of tabulated frequency responses

Original
Causality-constrained interpolation of tabulated frequency responses / Triverio, Piero; GRIVET TALOCIA, Stefano. - STAMPA. - (2006), pp. 181-184. (Intervento presentato al convegno IEEE 15th Topical Meeting on Electrical Performance of Electronic Packaging tenutosi a Scottsdale, AZ (USA) nel 23-25 Oct. 2006) [10.1109/EPEP.2006.321223].

Availability:
This version is available at: 11583/1647208 since:

Publisher:
IEEE

Published
DOI:10.1109/EPEP.2006.321223

Terms of use:

This article is made available under terms and conditions as specified in the corresponding bibliographic description in the repository

Publisher copyright

(Article begins on next page)

19 April 2024

2006 IEEE Electrical Performance of Electronic Packaging

Causality-constrained interpolation of tabulated frequency responses

P. Triverio, S. Grivet-Talocia

Dip. Elettronica, Politecnico di Torino, C. Duca degli Abruzzi 24, 10129 Torino, Italy

Ph. +39 011 5644005, Fax +39 011 5644099 (e-mail piero.triverio@polito.it)

Abstract: We apply a recently developed formulation of the generalized Hilbert transform to the processing of tabulated and finite-bandwidth frequency responses. A causality-constrained interpolation procedure is introduced, with the aim of reconstructing missing samples in the data, like e.g. the DC point, via a sound numerical procedure that does not compromise the self-consistency and the causality of the entire dataset.

1 Introduction and motivations

It is widely recognized that modeling and simulation of electrical interconnect parts of modern electronic systems is a very challenging task, which in several cases still lacks of appropriate solutions. Both academic and industry research in this field is very active, aiming at characterization, modeling, and simulation methods allowing to deal with the everincreasing system complexity at chip, package, and board level.

Electrical interconnects are linear structures. Therefore, a frequency-domain characterization is highly desirable. Such characterization can be obtained via full-wave electromagnetic simulation or direct measurement. In both cases, the result is a set of frequency samples over a finite bandwidth for some transfer matrix (scattering, impedance, or admittance) of the structure. Practically any EDA or CAD tool uses this frequency-domain characterization for subsequent modeling steps, including time-domain conversion or macromodeling for handling nonlinear terminations.

Very often the available frequency samples are affected by the presence of missing data points. A typical case is the missing DC (zero-frequency) point in VNA measurements or in simulation results obtained by frequency-domain tools. This issue may be very critical, since the zero-frequency point controls the DC steady state of the electrical solution, which is of paramount importance in any system design. Therefore, this problem is usually circumvented by applying suitable interpolation/extrapolation schemes in order to "fill the gaps" in the data. Linear or spline-based schemes are very common. However, the employment of such schemes for data recovery introduces some degree of arbitrarity in the computed samples, and it may be difficult to otbain an estimate for the error that is thus introduced in the structure characterization. In [1], we show that accuracy is not even the most important aspect. In fact, when some frequency points are affected by such errors, the overall frequency response may be inconsistent and flawed by causality violations. This has a dramatic impact, since non-causal data are also non-passive and will very likely induce a failure when attempting subsequent modeling or macromodeling steps. An illustrative example is reported in [1].

In this work, we provide a solution for this problem. We apply the generalized Hilbert transform to the design of a causality-constrained interpolation scheme. The main algorithm is based on a robust numerical procedure and allows to estimate the missing data points by explicitly enforcing the causality of the resulting dataset. We show that the proposed scheme produces far more accurate samples than common basic interpolation schemes. In addition, the guarantee of causality allows blind and safe application of standard modeling or macromodeling techniques. This applies to both lumped and distributed interconnect structures.

The paper is organized as follows. Section 2 reviews the generalized Hilbert transform and outlines a robust numerical procedure for its evaluation. Section 3 details the proposed causal interpolation algorithm. Finally, some application examples are presented in Section 4.

2 Generalized Hilbert transform

We consider a generic linear system with input-output behavior described by

$$y(t) = h(t) * x(t) \xrightarrow{\mathscr{F}} Y(j\omega) = H(j\omega)X(j\omega) \tag{1}$$

with $x(t)$, $y(t)$, and $h(t)$ being respectively the input, output and impulse response, observed in time-domain. Capital quantities denote their Fourier transforms, with $H(j\omega)$ being the system frequency response. Throughout this work, the real and imaginary parts of $H(j\omega)$ will be denoted as $U(\omega)$ and $V(\omega)$, respectively. Without loss of generality, we restrict our attention to a scalar $H(j\omega)$, i.e. to single-input single-output systems. However, the proposed methodology can be extended to multiport systems by considering each element of the matrix $\mathbf{H}(j\omega)$ separately.

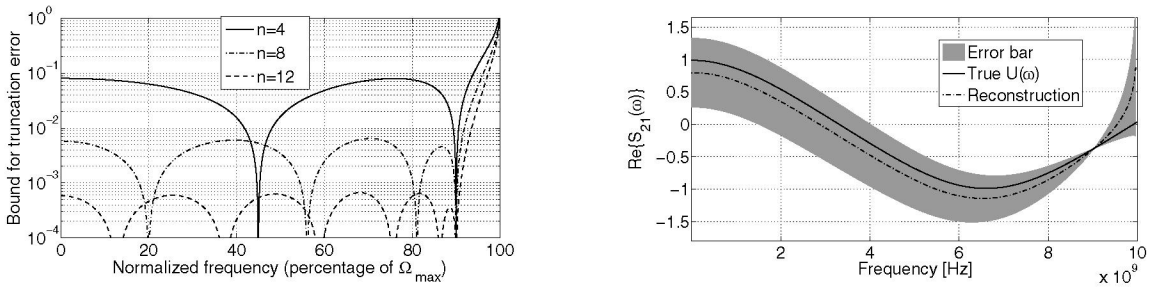

Figure 1: Left: truncation error bound $T_n(\omega)$ for $n = 4$, 8, and 12 subtraction points. Right: $\mathbb{R}\mathrm{e}\{S_{21}\}$ (solid line) for a transmission line (L=5.2 nH/cm, C=1.1 pF/cm, R=1.3 Ω/cm, G=0, length l=1 cm) and its numerical reconstruction (dash-dot line) obtained with (5). The shaded area accounts for the errors associated with the computation of (5).

A strong relationship between the real and imaginary parts $U(\omega)$ and $V(\omega)$ of any frequency response is established by the causality principle, which states that in every physical system the output reaction cannot precede in time its cause, i.e. the input variation. It is well known in fact that $U(\omega)$ and $V(\omega)$ are related by Kramers-Krönig dispersion relations [2] or, equivalently, by the Hilbert transform [3]

$$U(\omega) = \frac{1}{\pi} \fint V(\omega') \frac{d\omega'}{\omega - \omega'}, \qquad V(\omega) = -\frac{1}{\pi} \fint U(\omega') \frac{d\omega'}{\omega - \omega'}. \tag{2}$$

The integrals are defined according to Cauchy's principal value and throughout the paper are supposed to extend from $-\infty$ to $+\infty$, unless differently noted. These relations are fully equivalent to causality and can be exploited, e.g., to verify the causality of a given frequency response or to reconstruct the real part from the imaginary one and viceversa.

The effectiveness of the above procedures is limited in practice because frequency data obtained either via measurement or simulation consist of a set of discrete points

$$H(j\omega_k), \qquad k = -K, \ldots, +K, \qquad \omega_{\pm K} = \pm\Omega_{\max} \tag{3}$$

spanning a limited frequency bandwidth $[-\Omega_{\max}, \Omega_{\max}]$, negative frequencies being known from basic spectrum symmetries. The numerical computation of (2) is therefore affected by two sources of inaccuracy, one being related to the discrete nature of the data (discretization error), and the other to the unavoidable restriction of the integrals to the available bandwidth (truncation error). To overcome these issues, a robust and accurate method to compute dispersion relations has been introduced in [1, 4]. The technique is based on a generalized formulation of the Hilbert transform, which is reported below for the real part only, with a similar relation holding for $V(\omega)$,

$$U(\omega) = \mathcal{L}_U(\omega) + \frac{\prod_{q=1}^{n}(\omega - \bar{\omega}_q)}{\pi} \fint \boxed{\frac{V(\omega') - \mathcal{L}_V(\omega')}{\prod_{q=1}^{n}(\omega' - \bar{\omega}_q)}} \frac{d\omega'}{\omega - \omega'}, \quad \mathcal{L}_X(\omega) = \sum_{q=1}^{n} X(\bar{\omega}_q) \prod_{\substack{p=1 \\ p\neq q}}^{n} \frac{\omega - \bar{\omega}_p}{\bar{\omega}_q - \bar{\omega}_p}. \tag{4}$$

In this expression, known in physics as *dispersion relation with subtractions* [2], the points $\{\bar{\omega}_q\}_{q=1}^{n}$ are called *subtraction points*; $\mathcal{L}_U(\omega)$ and $\mathcal{L}_V(\omega)$ are the Lagrange interpolation polynomials, based on these points, for $U(\omega)$ and $V(\omega)$ respectively. Equation (4) can be obtained if (2) is applied to $U(\omega)$ and $V(\omega)$ diminished by their Lagrange interpolation polynomials, and then divided by $\prod_{q=1}^{n}(\omega - \bar{\omega}_q)$ (boxed quantity). This division is the key advantage of the generalized Hilbert transform, because it strongly reduces the importance of the missing high-frequency data $H(j\omega)$ for $|\omega| > \Omega_{\max}$.

Application of (4) to tabulated data (3) leads to an approximate numerical reconstruction of the frequency response real part

$$\hat{U}(\omega) = \mathcal{L}_U(\omega) + \frac{\prod_{q=1}^{n}(\omega - \bar{\omega}_q)}{\pi} \fint_{-\Omega_{\max}}^{+\Omega_{\max}} \frac{V(\omega') - \mathcal{L}_V(\omega')}{\prod_{q=1}^{n}(\omega' - \bar{\omega}_q)} \frac{d\omega'}{\omega - \omega'}, \tag{5}$$

which is affected by both discretization and truncation errors. In [1, 4] two worst-case bounds for these errors (denoted here as $\tilde{D}(\omega)$ and $T_n(\omega)$, respectively) are derived. We report as an example the maximum truncation error for the scattering parameters of a passive structure

$$T_n(\omega) = \frac{1}{\pi} \sum_{q=1}^{n} \left[\left| \ln \frac{\Omega_{\max} - \bar{\omega}_q}{\Omega_{\max} - \omega} \right| - (-1)^n \left| \ln \frac{\Omega_{\max} + \bar{\omega}_q}{\Omega_{\max} + \omega} \right| \right] \prod_{\substack{p=1 \\ p\neq q}}^{n} \frac{|\omega - \bar{\omega}_p|}{\bar{\omega}_q - \bar{\omega}_p}, \tag{6}$$

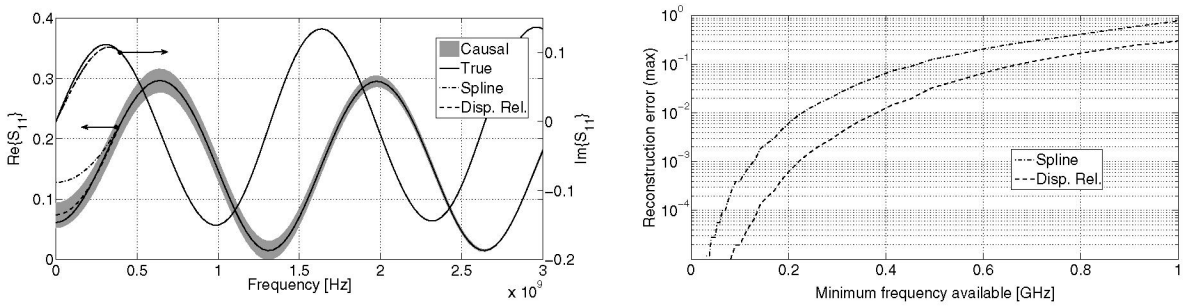

Figure 2: Left: true S_{11} (solid line), its reconstruction with spline interpolation (dash-dot lines), and with dispersion relations (dashed lines). The shaded area represents the bounds on the real part imposed by the dispersion relations. Right: maximum reconstruction error for conventional (dash-dot line) and proposed scheme (dashed line).

showing its behavior in Figure 1 (left) for $n = 4$, 8, and 12 subtractions. The rapid decrease of the truncation error for increasing n visible in the plot has an important consequence: with the proposed generalized dispersion relations (5), the numerical error due to the intrinsic bandwidth limitation can be arbitrarily reduced by choosing an appropriate number n of subtraction points.

Since the maximum uncertainty that affects (5) has been estimated as $|\hat{U}(\omega) - U(\omega)| \leq T_n(\omega) + \tilde{D}(\omega)$, an error bar accounting for the numerical resolution of the computation can be associated to $\hat{U}(\omega)$. Its importance is demonstrated in Figure 1 (right), where the real part $U(\omega)$ of the S_{21} scattering coefficient for a transmission line is depicted, together with $\hat{U}(\omega)$ obtained by applying (5). The frequency data have been supposed known only up to 10 GHz. Since the transmission line is a causal system, we expect dispersion relations to be satisfied, i.e. that $\hat{U}(\omega)$ matches $U(\omega)$: this would not be evident from Figure 1, unless one considers the uncertainty associated to $\hat{U}(\omega)$, represented in the graph by the shaded area that surrounds the dash-dot line. The dataset is concluded to be causal since the true response $U(\omega)$ is uniformly within the uncertainty bounds. Further details on the robust computation of dispersion relations can be found in [1, 4], where they are used for causality verification purposes; in the next section, their application for frequency data reconstruction is discussed.

3 Causality-constrained interpolation

We consider a tabulated frequency response as in (3) for which data are missing for $|\omega| < \Omega_{\min}$. Our aim is to recover the missing samples with the maximum achievable accuracy. The standard approach to this problem resorts to conventional interpolation procedures (i.e. splines): the real and imaginary parts are interpolated separately in $[-\Omega_{\min}, \Omega_{\min}]$ in order to compute a reconstructed response $H_R(j\omega) = U_R(\omega) + jV_R(\omega)$ that extends the given $H(j\omega)$ to the entire bandwidth $[-\Omega_{\max}, \Omega_{\max}]$. Two main drawbacks affect this procedure: low accuracy and non-causality of the reconstruction, as illustrated by the following example. The S_{11} scattering parameter of the same transmission line in Fig. 1 (now with length l=5 cm) has been computed from 0.4 up to 10 GHz. Then, spline interpolation has been used to reconstruct the frequency response for $f < 0.4$ GHz. The result is depicted in the left panel of Figure 2 (dash-dot lines), together with the true frequency response (solid lines). The reconstruction near $f = 0$ is very inaccurate and non-causal. In fact, application of the causality check tool introduced in [1, 4] clearly highlights this causality violation, since the reconstructed real part is outside the bounds (shaded area) imposed by the dispersion relations.

To overcome these issues, we propose the following methodology, which combines interpolation methods with dispersion relations. First, the imaginary part of (3) is interpolated in $[-\Omega_{\min}, \Omega_{\min}]$ to compute $V_R(\omega)$ using a conventional (e.g., spline) method. The imaginary part is preferred to the real part because its value for $f = 0$ is vanishing, owing to spectrum symmetries. Therefore, an additional point can be used in the interpolation, improving the overall accuracy of the method. Then, the dispersion relation (5) is applied to $V_R(\omega)$ in order to recover the real part $\hat{U}_R(\omega)$. Since the reconstructed response $H_R(j\omega) = \hat{U}_R(\omega) + jV_R(\omega)$ satisfies dispersion relations by construction, the causality of the result is always guaranteed. The superior accuracy of the proposed technique is now demonstrated.

We applied the reconstruction procedure to the same transmission line example above. The result of the proposed reconstruction scheme is depicted by dashed lines in Figure 2 (left). It is clear that the accuracy of the points below 0.4 GHz is far better than what is achievable with a standard interpolation. Moreover, the reconstruction is uniformly within the bounds imposed by dispersion relations, hence it is causal. The right panel of Figure 2 compares the deviation between interpolated and true response for both conventional and proposed causality-constrained schemes, as a function of $\Omega_{\min}$. The advantage of using dispersion relations is evident, since accuracy is improved by approximately one order of magnitude.

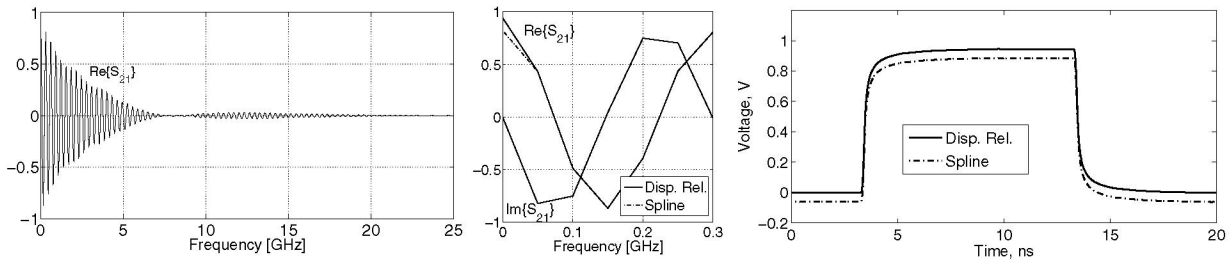

Figure 3: Left: $\mathbb{R}\mathrm{e}\,\{S_{21}\}$ of a measured 50 cm PCB interconnect. Middle: zoom on the low frequencies, comparing standard spline (dash-dot line) and causality-constrained (continuous line) reconstruction. Right: time-domain solution (obtained via inverse FFT) excited by a periodic pulse train, showing the DC shift between the two reconstruction methods.

We discuss now the placement of subtractions $\bar{\omega}_q$. Since truncation error is very small near subtraction points (see equation (6)), it is convenient to place them close to the bandwidth of interest $[-\Omega_{\min}, \Omega_{\min}]$. However, a minimum distance between subtractions has to be respected, in order to avoid an increased discretization error due to the excessive proximity of singularities in (5). Obviously, subtractions cannot be placed inside $[-\Omega_{\min}, \Omega_{\min}]$ where the real part $U(\omega)$ is not yet known, because its values $U(\bar{\omega}_q)$ are required in (5) to compute $\mathcal{L}_U(\omega)$. According to these considerations, we adopted the following rule

$$\{\bar{\omega}_q\}_{q=1}^{n} = \{\pm\Omega_{\min}(1+\alpha), \pm\Omega_{\min}(1+\alpha)^2, \ldots, \pm\Omega_{\min}(1+\alpha)^{n/2}\} \qquad \text{for } n \text{ even},$$

which provides a good compromise when $\alpha = 0.2 \div 0.3$. The number of subtractions n is chosen using (6) in order to guarantee a truncation error $T_n(\omega)$ smaller than a predefined threshold for $\omega \in [-\Omega_{\min}, \Omega_{\min}]$. Finally, we remark that the proposed causality-constrained interpolation scheme can be adapted with obvious modifications to the reconstruction of missing data intervals centered at any frequency, and not necessarily at $f = 0$.

4 Application examples

We consider now an application example. A single stripline routed over 50 cm on a PCB was measured from 50 MHz up to 40 GHz (courtesy of C. Schuster, IBM). The measured data account also for the discontinuities induced by the signal launches. The left panel of Fig. 3 depicts the real part of the insertion loss S_{21}, showing the significant phase rotations due to the length of the interconnect link. Both the standard (spline) and the proposed causality-constrained interpolation schemes were applied to compute an estimate of the missing DC point. The results are compared in the middle panel of Fig. 3, where an enlarged scale is used for the frequency axis. Due to the rather coarse sampling frequency, the two DC point estimates are quite different. Therefore, a dramatic impact on the transient solution of the link is expected.

In order to provide an unbiased check for the accuracy of the computed DC points (we do not have a reference point to compare with), we devised the following numerical test. The transient response of the interconnect was computed starting from the two different interpolated datasets. A repeated pulse with pattern `0111111111000000000`, bit time $T_b = 1$ ns and rise time $\tau_r = 130$ ps was applied, and the transient response was computed via inverse FFT. Special care was taken to avoid aliasing effects by smoothing the rise/fall edges of the input pulse. Also, ideal 50 Ω driver and receiver impedances were used. The results are compared in the right panel of Fig. 3. The transient solution computed using the causality-constrained dataset has a baseline DC solution around 0 V, as expected. Conversely, the spline-based dataset results in a DC shift, which can be quantified in about -60 mV. This simple example clearly points out that simplistic solutions to the pre- or post-processing of data may have a quite significant impact on subsequent modeling and simulation steps. Therefore, particular care should be taken in data conditioning, with particular emphasis on fundamental properties such as causality and passivity.

References

[1] P. Triverio and S. Grivet-Talocia, "A robust causality verification tool for tabulated frequency data," in *10th IEEE Workshop on Signal Propagation on Interconnects, Berlin, Germany*, May 9–12, 2006.

[2] N. M. Nussenzveig, *Causality and dispersion relations.* Academic Press, 1972.

[3] S. L. Hahn, "Hilbert transforms," in *The Transforms and Applications Handbook*, A. D. Poularikas, Ed. CRC and IEEE, 2000.

[4] P. Triverio and S. Grivet-Talocia, "On checking causality of bandlimited sampled frequency responses," in *2nd Conference on Ph.D. Research in Microelectronics and Electronics (PRIME), Otranto (LE), Italy*, June 12–15, 2006, pp. 501–504.